Using computational fluid dynamics for different alternatives water flow path in a thermal photovoltaic (PVT) system

S. Hoseinzadeh[1,*], Ali Sohani[2], Saman Samiezadeh[3], H. Kariman[4], M.H. Ghasemi[5]

[1]Department of Mechanical and Aeronautical Engineering, University of Pretoria, Pretoria, South Africa
[2]Faculty of Mechanical Engineering-Energy Division, KN Toosi University of Technology, Tehran, Iran
[3]School of Automotive Engineering, Iran University of Science and Technology, Tehran, Iran
[4]Faculty of Mechanical and Energy Engineering, Shahid Beheshti University, Tehran, Iran
[5]Department of Mechanical Engineering, West Tehran Branch, Islamic Azad University, Tehran, Iran

*Corresponding author
Siamak Hoseinzadeh can be contacted at: hoseinzadeh.siamak@gmail.com

Abstract

Purpose: This study aim to use the finite volume method to solve differential equations related to three-dimensional simulation of a solar collector. Modeling is done using ANSYS-fluent software program. The investigation is done for a photovoltaic (PV) solar cell, with the dimension of 394 × 84 mm^2, which is the aluminum type and receives the constant heat flux of 800 $W.m^{-2}$. Water is also used as the working fluid, and the Reynolds number is 500.

Design/methodology/approach: In the present study, the effect of fluid flow path on the thermal, electrical and fluid flow characteristics of a PV thermal (PVT) collector is investigated. Three alternatives for flow paths, namely, direct, curved and spiral for coolant flow, are considered, and a numerical model to simulate the system performance is developed.

Findings: The results show that the highest efficiency is achieved by the solar cell with a curved fluid flow path. Additionally, it is found that the curved path's efficiency is 0.8% and 0.5% higher than that of direct and spiral paths, respectively. Moreover, the highest pressure drop occurs in the curved microchannel route, with around 260 kPa, which is 2% and 5% more than the pressure drop of spiral and direct.

Originality/value: To the best of the authors' knowledge, there has been no study that investigates numerically heat transfer, fluid flow and electrical performance of a PV solar thermal cell, simultaneously. Moreover, the effect of the microchannel routes which are considered for water flow has not been considered by researchers so far. Taking all the mentioned points into account, in this study, numerical analysis on the effect of different microchannel paths on the performance of a PVT solar collector is carried. The investigation is conducted for the Reynolds number of 500.

Keywords: Comparative study, Energy efficiency, Numerical simulation, Photovoltaic thermal (PVT) system, Water flow path

Nomenclature

A = area (m^2);
a = coefficient in the discretization equation;
c = specific heat ($J.kg^{-1}.K^{-1}$);
C_p = specific heat at constant pressure ($J.kg^{-1}.K^{-1}$);
D = diffusion conductance ($kg.s^{-1}$);
D_h = hydraulic diameter;
E_c = absorbed energy by PV cell (J);
E_{ce} = produced energy by PV cell (J);
F = convection mass flux ($kg.s^{-1}$);
$G(t)$ = solar radiation ($W.m^{-2}$);
h = convective heat transfer coefficient ($W.m^{-2}.K^{-1}$);
K = thermal conductivity ($W.m^{-1}.K^{-1}$);
m = mass (kg);
n = normal vector;
Nu = Nusselt number;
P = wetted perimeter (m);
Q = energy transfer (J);
q_c = convection heat transfer (W);
$\dot{q}$ = rate of energy generation ($W.m^{-3}$);
Re = Reynolds number;
S = general source term;
$\overline{S}$ = average value of source term;
S_p = coefficient of ϕ_P in the linearized source expression;
S_u = constant part of average value of source term;
T = temperature (K);
$T_a(t)$ = temperature of air flow (K);
T_b = temperature of backsheet (K);
t = time (s);
u = velocity vector ($m.s^{-1}$);
V = volume (m^3);
V_d = displacement volume (m^3); and
x, y, z = Coordinates.

Scripts

E = neighbor in the positive $\times$ direction, i.e. on the east side;
e = control volume face between P and E;
in = inlet flow;
m = mean;
N = neighbor in the positive y direction, i.e. on the north side;
n = control volume face between P and N;
out = outlet flow;

P = central grid point under consideration;
p = packing factor;
pa = panel;
ref = reference;
S = neighbor in the negative y direction, i.e. on the south side;
s = control volume face between P and S;
W = neighbor in the negative $\times$ direction, i.e. on the west side; and
w = control volume face between P and W.

Abbreviations

NOCT = nominal operating cell temperature;
SIMPLE = semi-implicit method for pressure linked equations;
PV = photovoltaic; and
PVT = photovoltaic thermal system.

Greek symbols

Δ = difference;
Γ = general diffusion coefficient;
ϕ = general dependent variable;
v = kinematic viscosity ($m^2.s^{-1}$);
ρ = density ($kg.m^{-3}$);
η_e = cell efficiency;
η_{el} = electrical efficiency;
τ_g = fraction transmitted through the front glass;
α_c = cell absorptivity; and
β = temperature coefficient (K^{-1}).

1. Introduction

A look at the backdrop of fossil fuel consumption is enough to reveal how critical is the status quo (Babaei et al., 2020). The use of fossil fuels has reached an unprecedented level in all human life (Razmi et al., 2018), and the danger of their depletion is so closer than any other time in the past (Doranehgard et al., 2017). Hence, alternative energy is necessary to reduce the cost of energy consumption (Zeynalian et al., 2020). In addition, it is vital to have a better condition from environmental pollution point of view (Razmi et al., 2019) because there have been increasing environmental concerns (Mohammadian et al., 2020). Among all the renewable energy sources, solar energy is ubiquitous and cheapest (Razmi and Janbaz., 2020), and during the recent years, they come into importance very much (Hoseinzadeh et al., 2020). The photovoltaic thermal (PVT) collectors as a type of solar energy technology are becoming more popular worldwide (Menni et al., 2019). These collectors produce thermal energy that can be used for different applications and, at the same time, generate electricity. In fact, they are similar to combined cooling, heating, and power (CCHP) systems (Sohani et al., 2020). PVT collectors can act as a cooling system for the PV systems to improve electrical efficiency. These collectors consist of microchannels, PV cells and manifold (Shashikumar et al., 2018). There are different types of PVT collectors, such as PVT water and air collectors. In water-type PVT collectors, water is heated when it passes through the cooling path (Manokar et al., 2020). There are several modes for fluid flow; the most important are direct, curve and spiral. Selecting an appropriate fluid path to obtain the maximum amount of radiation energy and cooling of the cell is very important (Hoseinzadeh et al., 2018).

Teo et al. (2012) obtained both thermal and electrical energies from the hybrid PVT system. The results of the experiments indicated that the use of a cooling system could be very effective. Under conditions where no coolant was used, the PV system temperature reached 68°C, and the system's electrical efficiency was significantly reduced and reached 8.6%. Using the air blower to cool the PV module, the PV module temperature can be maintained at 38°C, and the electrical efficiency is about 12.5%.

Xu et al. (2015) and Yu et al. (2018) showed that the new heat sink microchannel consisted of longitudinal parallel microchannels and several transverse microchannels to separate the total flow length to different points. The entire length of the parallel microchannels in the longitudinal direction was 21.245 mm, and the total width of the cover of the triangular microchannel was 4.35mm with a hydraulic diameter of 155µm. The microchannel was made of silicon and a thin film of platinum was deposited by chemical vapor using the sedimentation method, yielding a uniform heat flux. In the experiments, they used ten triangular longitudinal parallel microchannels and five transverse trapezoidal microchannels.

In the references Agrawal and Tiwari (2011, 2015) Agrawal and Tiwari investigated the parallel routes of solar cells by passing air below them for cooling. In this study, nine rows of solar cells were arranged together all in a column, resulting in four columns of solar cells in parallel. For cooling the solar cells, the air was used with microchannels, and four air paths were considered in this study. Different routes were used to pass the airflow. In this study, a radiant intensity of 700W.m^{-2} was radiated to the surface of the cells. The results of this study showed that the electrical and electrical efficiency of the paths were different, so that choosing a suitable route to enhance the thermal and electrical efficiency was of great importance to the set.

Valadez-Villalobos et al. (2019) theoretically studied the performance of PV solar cells at high temperatures. They confirmed that the voltage in the open circuit was reduced with the temperature and concluded that the main factor in reducing productivity was the decrease in the open-circuit voltage. They studied the effect of light concentration on cell parameters at 300 K. They concluded that the increase in the short-circuit current was much more severe than in the open-circuit voltage.

In two studies Coventry et al. (2005, 2015) Coventry et al. achieved advances in an analytical method to predict the temperature distribution in a PV cell. They assumed that the surface had a uniform temperature and that light would be radiated uniformly on different parts. The results showed that the high non-uniform temperature in the cells, because of the high heat produced by non-uniform radiation, could cause a temperature drop of up to 36.4°C.

Two investigations were also carried out by Fudholi et al. in Fudholi et al. (2014, 2015). They placed a PVT device exposed to radiation for one day from 8 a.m. to 5.30 p.m. They found that the system's maximum performance was around 13 o'clock, in which the collector outlet temperature, the cell temperature and the ambient temperature were 53.2°C, 70.3°C and 37°C, respectively. They also found that the electrical and thermal efficiency of the system increased with decreasing ambient temperature, and up to a water flow rate of 0.01 kg.s^{-1}, the electrical and thermal efficiency were increasing and remained fixed for flow rates above this value.

Lee et al. (2006) conducted their study on a single microchannel. They changed the dimensions of the microchannel, so that the channel length to width was changed for ten modes, but its length was fixed at 120 mm. In this study, a ratio of $\alpha = \frac{b}{a}$ expressing the length to width ratio of the microchannel was used. In addition, the hydraulic diameter differed given dimension variation. Constant heat flux was applied to the upper surface of

the microchannel and the fluid flow passed through the microchannel, hence allowing heat transfer between the channel and the water and heating the water. Furthermore, it was observed that Nusselt variations that were started asymptotically from the beginning of the channel were high and decreased up to the end of the channel.

Ghale et al. (2015) conducted a study on a rectangular thermal solar microchannel. They used a number of 25 microchannels beneath a solar panel with a thermal flux applied to them. The fluid entered the channels on one side and left on the other side. In this study, the effect of temperature and thermal flux in different Reynolds numbers on the Nusselt numbers and the pressure drop inside the microchannel was investigated using the computational fluid dynamics. The results of this study indicated that the fluid temperature was lower and higher at the points near the wall and in the central points, respectively. Moreover, with increasing thermal flux from 100 to 400 $W.m^{-2}$, the Nusselt number and the pressure drop increased and decreased, respectively, as 32% and 14%. Furthermore, with the increase in the Reynolds number, the changes in the Nusselt number increased for a radiant intensity.

The studies done by Nader Rahbar et al. in the references such as Rahbar and Esfahani (2013), Rahbar et al. (2015, 2016) can be given as other examples of the related studies to the topic of this paper. In those studies, the authors examined a flat solar collector, the bottom plate of which had rectangular blocks of V shape embedded as corrugated. The mass flow rate of the fluid inside the collector was adjusted between 0.003 and 0.01 $kg.s^{-1}$ by a centrifuge fan and the Reynolds number within the channel was set between 1,000 and 3,500. The device was placed at 30°–45° and 90°. The study findings revealed that the output air temperature of the device was relatively independent of the angle of position of the device and was the same in all cases. In addition, the Nusselt number on the V-shaped plate was more than five times of the Nusselt number on the flat plates, and the device efficiency increased in comparison with the improved flat plates. They also proposed a new relation for the average Nusselt number as $\overline{Nu} = 0.998\mathrm{Re}^{0.5233}$.

As another point about reviewing the literature, it should be noted that for the numerical modeling of the performance of PVT systems, semi-implicit method for pressure linked equations (SIMPLE) method has been one of the most popular ones. The SIMPLE method has been widely used in different studies for different systems. The studies of (Abdollahzadeh Jamalabadi et al., 2017), (Hoseinzadeh et al., 2019), (Chien et al., 2020), (Chamkha et al., 2017), (Yan et al., 2019), (Bahiraei et al., 2019), (Salehi et al., 2020), (Yarmand et al., 2014), (Ghalambaz et al., 2017), (Hosseinzadeh et al., 2017), (Rahmanian et al., 2014) and (Garoosi et al., 2015) can be given as some examples that show the broad range of application and capability of SIMPLE method.

A quick review of the studies have been done on the analysis of solar collectors in different aspects (e.g. thermal performance), which is presented in Table 1. Despite valuable studies done so far in this field, there have been shortcomings that should be addressed. There are some questions in Table 1, which provide a clear insight regarding the novelty of this research.

As observed in the literature of Table 1, as well as the performed literature review, to the best of our knowledge, there has been no study to investigate heat transfer, fluid flow and electrical performance of a PV solar thermal cell numerically, simultaneously. Moreover, the effect of the microchannel routes, which are considered for water flow, has not been considered by researchers so far. By considering all the mentioned points, in this study, numerical analysis of the effect of different microchannel paths on the performance of a PVT solar collector is carried out. The investigation is done for the Reynolds number of 500.

Table 1. List of the related studies done in the field recently

Study	Year	Was a numerical model to predict the performance of the system developed?	If so, were the electrical, energy and fluid flow criteria considered simultaneously?	Was a comparative study conducted among different alternatives for water flow?	If so, did the investigation take all the important performance indicators, such as electrical, mechanical and heat transfer ones at the same time?
Coventry *et al.* (2004)	2004	No	No	No	No
Xu *et al.* (2005)	2005	No	No	No	No
Coventry (2005)	2005	No	No	No	No
Meneses-Rodriguez *et al.* (2005)	2005	Yes	No	No	No
Lee *et al.* (Lee and Garimella., 2006)	2006	Yes	No	No	No
Agrawal *et al.* (Agrawal and Tiwari, 2011)	2011	No	No	No	No
Teo *et al.* (2012)	2012	No	No	No	No
Rahbar *et al.* (Rahbar and Esfahani, 2013)	2013	Yes	No	No	No
Fudholi *et al.* (2014)	2014	No	No	No	No
(Xu *et al.*, 2015)	2015	Yes	No	No	No
Agrawal *et al.* (Agrawal and Tiwari, 2015)	2015	No	No	No	No
Fudholi *et al.* (2015)	2015	No	No	No	No
Ghale *et al.* (2015)	2015	Yes	No	No	No
Rahbar *et al.* (2015)	2015	Yes	No	No	No
Rahbar *et al.* (2016)	2016	No	No	No	No
Yu *et al.* (2018)	2018	No	No	No	No
Valadez-Villalobos *et al.* (2019)	2019	Yes	No	No	No
The current study	*2020*	*Yes*	*Yes*	*Yes*	*Yes*

2. Investigated geometry

Parameters of geometry, including both heat sink and microchannel dimensions, are shown in Figure 1. The length, width and height of the heat sink are 393, 165 and 15 mm, respectively. Moreover, 23 microchannels with a height of 0.15mm and a width of 0.5mm are used in this study. Also, the wall thickness between adjacent channels is 2.5 mm. The cover plate with a height of 7mm is made from aluminum and serves as a solar cell and the collector's entrance. The three fluid flow paths including direct, curved and spiral are considered for the PV collector's microchannel. The angle of inclination of the solar collector is fixed because of the limit on the solar cell dimension.

3. Numerical simulation

Defining a problem plays a vital role in obtaining accurate results. The details about numerical simulation are presented in this section. It contains general information, boundary conditions, equations and a brief description of the method used.

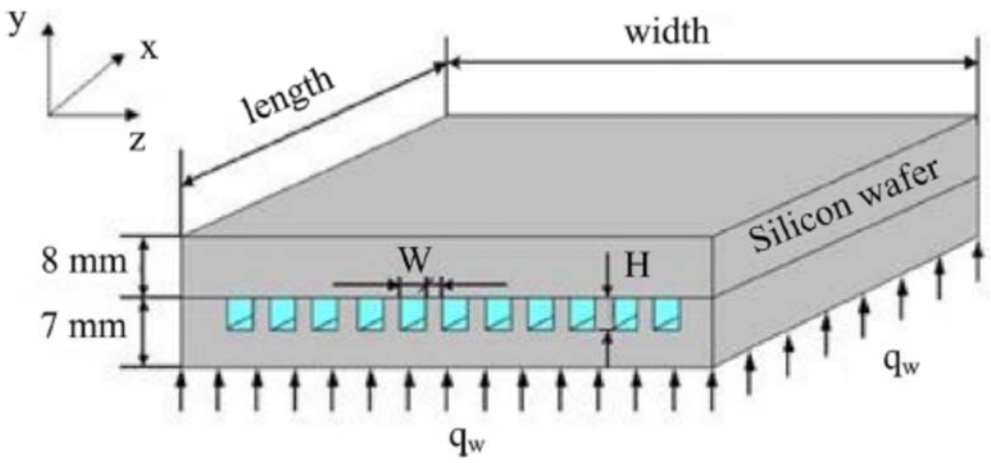

Figure 1. Schematic of the considered geometry; the illustration is similar to the study by Li et al. (2004), but the dimensions have been changed

3.1 General information

The problem assumptions used to analysis of heat transfer in the PV solar cell are as follows:

- the process is steady-state and steady flow;
- constant and steady heat flux is applied to the upper wall of the microchannel;
- the effect of radiation heat transfer inside the fluid and between the fluid and its surroundings is neglected;
- the heat flux from the microchannel bottom insulated wall is zero; and
- the coolant flow is single-phase, steady, laminar and incompressible.

Given the heat flux in the microchannels, the heat transfer occurs between the coolant passing through the microchannel and aluminum plate.

3.2 Boundary conditions

As discussed before, the flow of the coolant is laminar. Reynolds number for laminar flow in the pipe or channel is less than 2,300. The constant thermal flux of 800 $W.m^{-2}$ is applied to the microchannel's upper surface, heating the fluid up. This value is selected because it is the reference condition for irradiation in the nominal operating cell temperature (NOCT) approach (Sohani et al., 2020). As it has been indicated in the literature, NOCT is the most common approach to determine the performance of a PV solar cell (Sohani and Sayyaadi., 2020). The heated coolant enters the collector after leaving the microchannel. The solar collector consists of a PV panel, aluminum cover, microchannel and manifold. All plates used in the solar collector are insulated. The water is considered as a coolant, and the metal used in the PV panel is aluminum.

3.3 Equations

The governing equations of the fluid flow which describe the physics of the problem are

Table 2. Equations related to the numerical method used in this

Equation	Equation no.	Ref	Description
$\frac{\partial}{\partial x}\left(K\frac{\partial T}{\partial x}\right)+\frac{\partial}{\partial y}\left(K\frac{\partial T}{\partial y}\right)+\frac{\partial}{\partial z}\left(K\frac{\partial T}{\partial z}\right)+\dot{q}=\rho c\frac{\partial T}{\partial t}$	(1)	Khodabandeh *et al.* (2019)	Heat diffusion equation
$h=\frac{Q}{A\cdot T_m}=\frac{C_p\dot{m}(T_{out}-T_{in})}{A[T_w-0.5(T_{in}-T_{out})]}\left[\frac{w}{m^2C^o}\right]$	(2)	Khodabandeh *et al.* (2019)	Equation related to conservation of energy
$div(\rho \mathbf{u}\phi)=div(\Gamma\ grad\ \phi)+S_\phi$	(3)	Yousef Nezhad and Hoseinzadeh. (2017)	The permanent diffusion–displacement equation by deleting the transient part
$\int_A \boldsymbol{n}\ .(\rho\phi\mathbf{u})dA=\int_A \boldsymbol{n}\ .(\Gamma\ grad\ \phi)dA+\int_{CV}\boldsymbol{n}\ .S_\phi dV$	(4)	Yousef Nezhad and Hoseinzadeh. (2017)	The flux balance in a control volume(total integral of equation (3) on the control volume)
$\frac{d}{dx}(\rho u\phi)+\frac{d}{dy}(\rho u\phi)=\frac{d}{dx}\left(\Gamma\frac{d\phi}{dx}\right)+\frac{d}{dy}\left(\Gamma\frac{d\phi}{dy}\right)+S$	(5)	Yousef Nezhad and Hoseinzadeh. (2017)	The normal diffusion and displacement of the property ϕ in a two-dimensional flow field
$[(\rho uA)_e\phi_e-(\rho uA)_wA_w]+[(\rho uA)_n\phi_n-(\rho uA)_sA_s]$ $=\left[\Gamma_eA_w\left(\frac{\partial\phi}{\partial x}\right)_e-\Gamma_wA_w\left(\frac{\partial\phi}{\partial x}\right)_w\right]+\left[\Gamma_nA_n\left(\frac{\partial\phi}{\partial y}\right)_n-\Gamma_sA_s\left(\frac{\partial\phi}{\partial y}\right)_s\right]+\overline{S}\Delta V$	(6)	Yousef Nezhad and Hoseinzadeh. (2017)	The integral of equation (5) on the control volume
$\Gamma_w=\frac{\Gamma_W+\Gamma_P}{2}\ (a),\ \Gamma_e=\frac{\Gamma_P+\Gamma_E}{2}\ (b)$ $\Gamma_n=\frac{\Gamma_N+\Gamma_P}{2}\ (c),\ \Gamma_s=\frac{\Gamma_P+\Gamma_S}{2}\ (d)$	(7a –7d)	Sarafraz *et al.* (2019)	Equations related to central difference method

(continued)

work

Equation	Equation no.	Ref	Description
$\Gamma_w A_w \left.\frac{\partial \phi}{\partial x}\right\|_w = \Gamma_w A_w \frac{\phi_P - \phi_W}{\delta x_{WP}} \quad (a)$, $\Gamma_e A_e \left.\frac{\partial \phi}{\partial x}\right\|_e = \Gamma_e A_e \frac{\phi_E - \phi_P}{\delta x_{PE}} \quad (b)$	(8a and 8 b)	Sarafraz *et al.* (2019)	Equation related to the flux passing through the control volume (western and eastern surfaces)
$\Gamma_s A_s \left.\frac{\partial \phi}{\partial y}\right\|_s = \Gamma_s A_s \frac{\phi_P - \phi_S}{\delta x_{SP}} \quad (c)$, $\Gamma_n A_n \left.\frac{\partial \phi}{\partial y}\right\|_n = \Gamma_n A_n \frac{\phi_N - \phi_P}{\delta x_{PN}} \quad (d)$	(8c and 8d)	Sarafraz *et al.* (2019)	Equation related to the flux passing through the control volume (southern and northern surfaces)
$\overline{S}\Delta V = S_u + S_P \phi_P$	(9)	Sarafraz *et al.* (2019)	Spring term in equation (6)
$F = \rho u A$	(10)	Sarafraz *et al.* (2019)	Convection mass flux displaced
$D = \frac{\Gamma A}{\delta}$	(11)	Sarafraz *et al.* (2019)	Diffusion conductance
$F_w = (\rho u A)_w (a), F_e = (\rho u A)_e (b), F_s = (\rho u A)_s (c), F_n = (\rho u A)_n (d)$	(12a)–(12d)	Sarafraz *et al.* (2019)	The mass flux associated with cell surfaces
$D_w = \frac{\Gamma_w}{\delta x_{WP}} (a), \quad D_e = \frac{\Gamma_e}{\delta x_{PE}} (b), \quad D_s = \frac{\Gamma_s}{\delta y_{SP}} (c),$ $D_n = \frac{\Gamma_n}{\delta x_{PN}} \quad (d)$	(13a–(13d)	Sarafraz *et al.* (2019)	The diffusion conductance associated with cell surfaces
$[F_e \phi_e - F_w \phi_w] + [F_n \phi_n - F_s \phi_s] = [D_e(\phi_E - \phi_P) - D_w(\phi_P - D_W)] + [D_n(\phi_N - \phi_P) - D_s(\phi_P - \phi_s)] + [S_u + S_p \phi_p]$	(14)	Sarafraz *et al.* (2019)	The diffusion–displacement equation
$\phi_w = \phi_W (a) \quad \phi_e = \phi_P (b)$	(15a) and (15b)	Yousef Nezhad and Hoseinzadeh. (2017)	Equations related to upwind differencing method
$[F_e \phi_P - F_w \phi_W] + [F_n \phi_P - F_s \phi_S] = [D_e(\phi_E - \phi_P) - D_w(\phi_P - \phi_W)] + [D_n(\phi_N - \phi_P) - D_s(\phi_P - \phi_s)] + [S_u + S_P \phi_P]$	(16)	Sarafraz *et al.* (2019)	Equation after applying the upwind scheme for equation (14)

(*continued*)

Equation	Equation no.	Ref	Description
$[(D_w + F_w) + (D_s + F_s) + D_e + D_n + (F_e - F_w) + (F_n - F_s) + S_P]\phi_P = (D_w + F_w)\phi_W + D_e\phi_E + (D_s + F_s)\phi_S + D_n\phi_N + S_u$	(17)	Sarafraz *et al.* (2019)	Equation after rewriting equation (16)
$a_P\phi_P = a_W\phi_W + a_E\phi_E$	(18)	Sarafraz *et al.* (2019)	Central coefficient equation related to upwind method
$a_P = a_W + a_E + (F_e - F_w)$	(19)	Sarafraz *et al.* (2019)	Central coefficient equation related to upwind method
$E_c = p\alpha_c\tau_g G(t)$	(20)	Bakhshi *et al.* (2019)	Absorbed radiation energy
$E_{ce} = \eta_e p\tau_g G(t)$	(21)	Bakhshi *et al.* (2019)	Electrical energy generated by the solar
$\eta_e = \eta_{ref}(1 - \beta(T - T_{ref})$	(22)	Bakhshi *et al.* (2019)	The electrical efficiency of the solar panel
$\eta_{el} = 0.147 - 0008T_{pa}$	(23)	Jaferian *et al.* (2019)	the electrical efficiency according to Teo and Lee (Teo *et al.*, 2012)
$q_c = h_c A_c[T_b - T_a(t)]$	(24)	Bergman *et al.* (2011)	Equation related to convective heat transfer
$q_c = mc[T_{out} - T_{in}]$	(25)	Bergman *et al.* (2011)	Equation related to convective heat transfer
$Re = \frac{VD_h}{v}$	(26)	Bergman *et al.* (2011)	Reynolds number
$D_h = \frac{4A}{P}$	(27)	Bergman *et al.* (2011)	Hydraulic diameter
$Nu_x = \frac{hD_h}{K_f}$	(28)	Bergman *et al.* (2011)	Nusselt number

introduced in this section. The finite volume method is used to solve the differential equations of the defined problem. Integrating on the grid domain generated through the boundary converts differential equations to the algebraic expressions in the finite volume method. It should be noted that the upwind differencing scheme is used to calculate the properties of the fluid (e.g. temperature). Also, the SIMPLE algorithm, which will be discussed in the following section, is used to calculate the pressure field of the fluid. All the equations used in this work to analyze heat transfer, fluid flow and electrical performance of a PV thermal collector are shown in Table 2. Moreover, to not make the paper so long, a brief description of the equations is presented in Table 2.

3.4 Semi-implicit method for pressure linked equations method

The SIMPLE method is used to determine pressure. The SIMPLE method is an efficient way to obtain the steady-state solution for heat transfer problems. Also, the computation time might be decreased using this algorithm. Its stepwise procedure makes the solution easier. This method has been used considering the equations related to laminar, steady and two-dimensional flow. In this algorithm, the disseized momentum equations are solved using the initial guess of flow values. Then, the uncorrected mass flux at faces is determined. After that, the pressure correction equation is solved to produce cell values of the pressure correction. Following this, the pressure field is updated. The next step is computing other flow variables (e.g. turbulence). Finally, if the solution converges, the algorithm is stopped; otherwise, the refined values are used as a new initial guess to solve the momentum equation again.

4. Results and discussion

This part includes validating the developed numerical simulation and comparing the three considered alternative paths for water from different aspects. It is worth mentioning that, as mentioned before, the comparisons are made for the Reynolds number of 500.

4.1 Validation of the developed numerical simulation

The current study is verified by the study of Peterson et al. (Li et al., 2004) regarding the three-dimensional analysis of heat transfer. The mentioned study was done according to geometry and microchannel dimensions shown in Figure 1, in which only some dimensions were not the same as this study.

As seen in Figure 2, a negligible difference between the simulation results and the study by Peterson (Li et al., 2004) is observed. The temperature variations for Reynolds numbers of 77 and 144 obtained are 40 and 17 K, respectively, when the developed numerical simulation is applied. A perfect agreement between the prediction of the developed numerical model and reported data of Peterson et al. (Li et al., 2004), is observed.

Also, in Figure 3, the obtained values for the numerical simulation for Reynolds numbers of 77 and 144 at the inlet velocity of 0.526 and 1.321 $m.s^{-1}$ are equal to 15 and 50 kPa, respectively. The maximum percentage difference of 1% between the present study and Peterson's study, i.e. 15.1 and 52.2 kPa, shows the accuracy of the simulation.

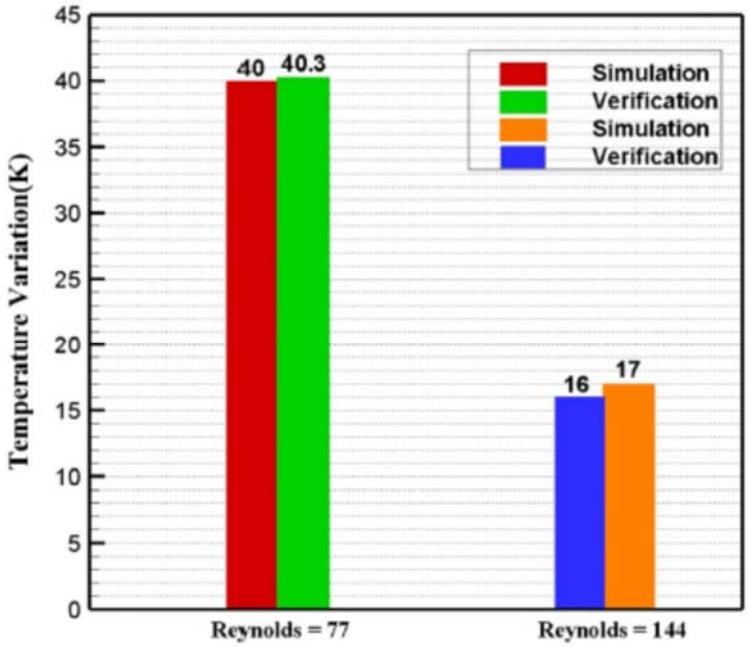

Source: Li *et al.* (2004)

Figure 2. Comparison of temperature variations between the current study and Peterson's study

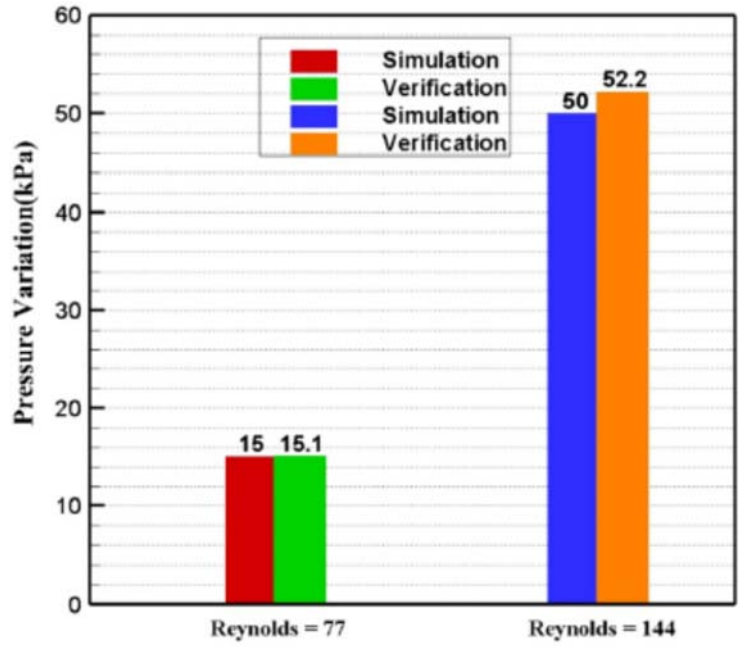

Source: Li *et al.* (2004)

Figure 3. Comparison of pressure variations between the current study and Peterson's study

4.2 Comparing different alternatives for flow path

Figure 4 shows the convergence points of solutions for three specified paths at the Reynolds number of 500. The SIMPLE algorithm was used in this simulation as mentioned before, to

determine pressure and velocity fields.

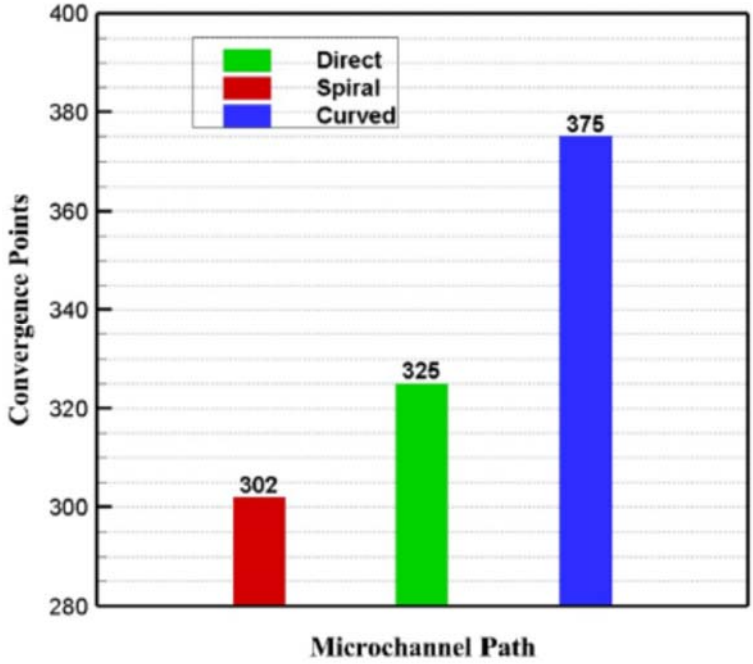

Figure 4. Convergence points at Reynolds number of 500

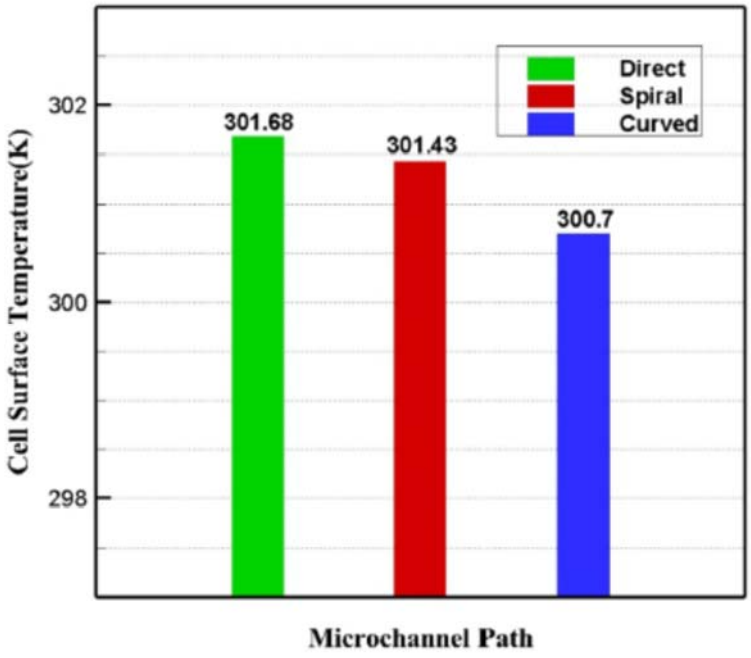

Figure 5. Temperature of cell surface at Reynolds number of 500

According to this figure, in the Reynolds number of 500, the value of convergence status for direct, spiral and curved paths is 302, 325 and 375, respectively. It means that the curved route's convergence points are 24%and 13% higher than that of the direct and spiral paths, demonstrates the solar cell surface temperature at Re = 500 for three microchannel routes of direct, curved and spiral. As seen in this figure, the highest temperature is related to the

direct path, 301.68 K, which is 0.08% and 0.32% more than the temperature of spiral and curved routes. The solar cell surface temperature for them is 301.43 and 300.7 K, respectively.

Based on the governing equations, the amount of absorbed energy in the solar cell depends on the plate absorption coefficient. The higher absorption is, the higher energy is absorbed. This energy heats the solar cell. According to Newton's Law of Cooling, convective heat transfer occurs between the heated solar cell and coolant of the system.

The length of the curved path is higher compared to other paths. It means that surface of heat exchange is more than other paths, leading to a higher reduction in the solar cell surface temperature compared to the other two paths.

Figure 6 indicates the differences between the temperature of inlet and outlet coolant at Reynolds number of 500 for the three paths. The temperature of inlet flow passing through the microchannel is considered to be 300 K. As discussed in the previous section, a constant heat flux is applied to the upper microchannel surface and coolant flow. The increase in the upper cross-sectional channel results in a higher temperature difference. The upper surface for the direct path is lower than the other paths. Therefore, the highest level of the temperature difference occurs for this path. According to Figure 6, at Reynolds number of 500, the temperature difference for fluid in the direct route is 1.68 K. Also, this amount for spiral and curved paths is 1.43 and 0.7 K, respectively. Hence, the temperature difference for fluid in the direct path is 17% and 58% more than that of spiral and curved path, respectively.

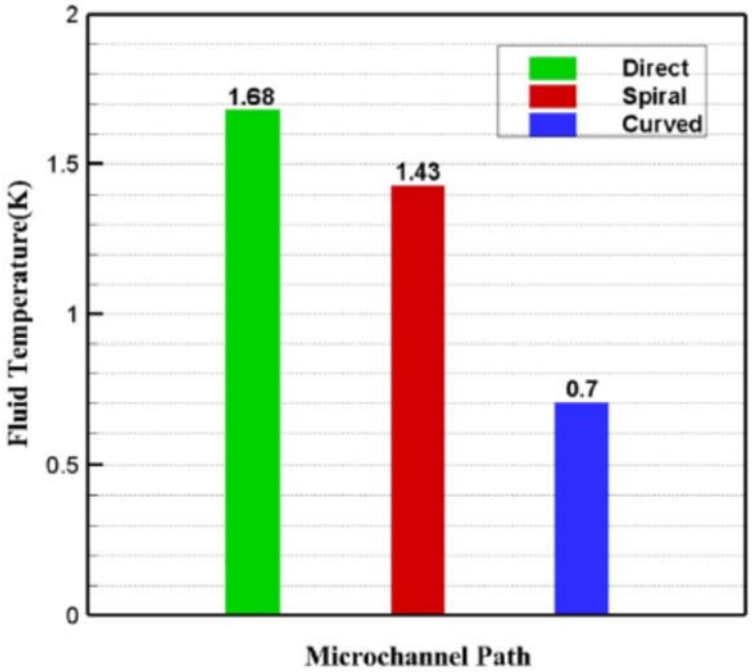

Figure 6. Temperature difference between fluid at outlet and inlet at Reynolds number of 500

The amount of Nusselt numbers at Re = 500 for three different microchannel paths is depicted in Figure 7. The convective heat transfer coefficient is a function of the difference in the surface and fluid temperature values. When the temperature difference decreases, the convection heat transfer coefficient and the Nusselt number increases. The temperature difference between the fluid walls for the curved path is lower than the other two paths because of the higher heat exchange surface compared to spiral and direct routes. At the Reynolds number of 500, the Nusselt numbers of 0.48, 0.63 and 0.72 are obtained for the direct, spiral and curved paths, respectively. This means the Nusselt number for the curved path is 14%and 50% higher than that of the spiral and direct paths, respectively.

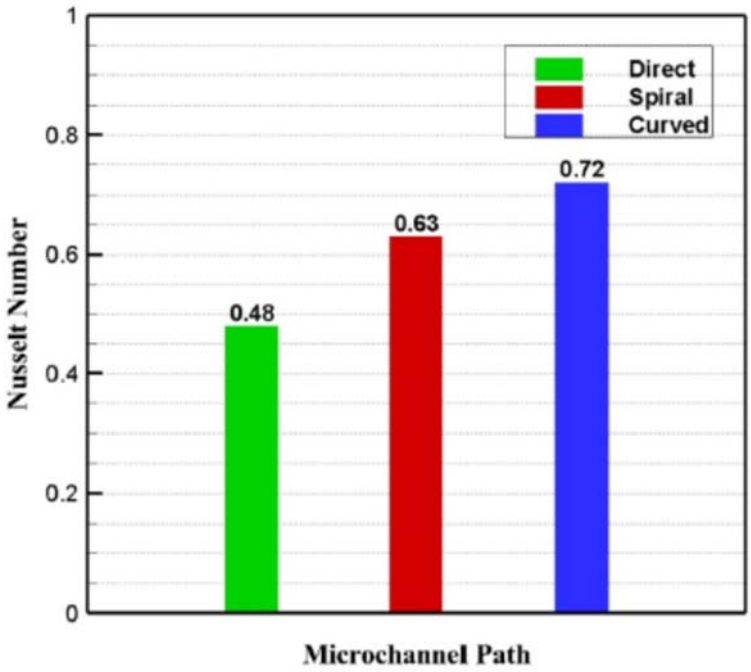

Figure 7. Nusselt number for three direct, spiral and curved paths at Reynolds number of 500

The electrical efficiency of the solar cell in three paths at Re = 500 is shown in Figure 8. Based on equation (22), the electrical efficiency increases with a reduction in the solar cell surface temperature. According to the results in Figure 5, the lowest cell surface temperature is related to the curve path. Therefore, the percentage of electrical efficiency in this path is higher in comparison to other paths. The obtained values of electrical efficiency for direct, spiral and curved paths are 12.28%, 12.42% and 12.48%, respectively. Therefore, at Re = 500, the electrical efficiency of the curved path is approximately 0.5% and 0.8% better than the electrical efficiencies of spiral and direct paths. Moreover, because of the higher heat exchange surface in the spiral path compared to the direct path, the electrical efficiency of the spiral path 0.32% is more than that of the direct path.

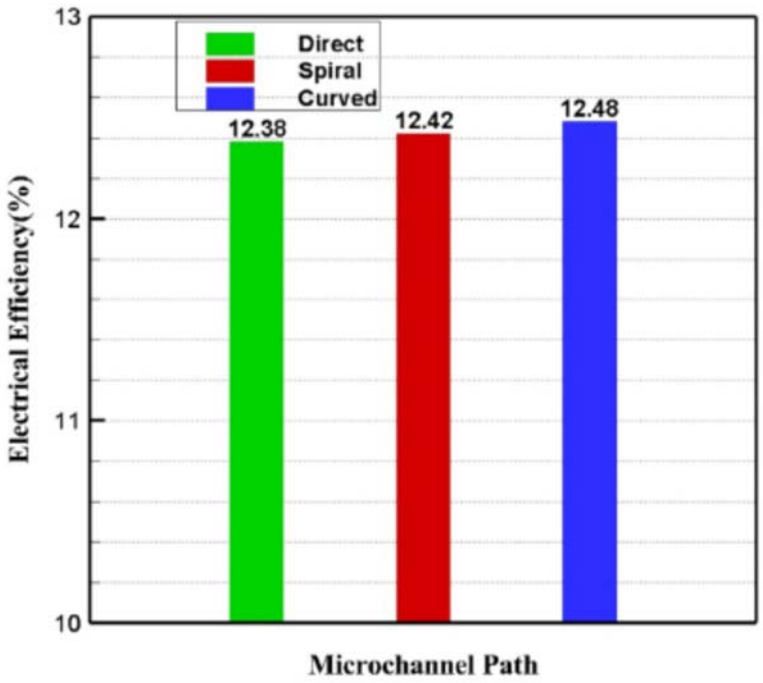

Figure 8. Electrical efficiency for three direct, spiral and curved paths at Reynolds number of 500

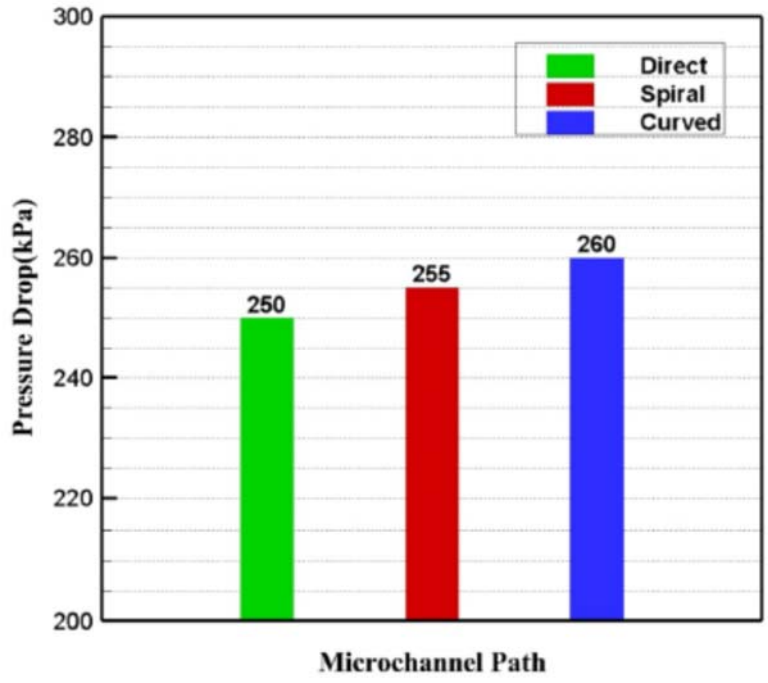

Figure 9. Pressure drop for three direct, spiral and curved paths at Reynolds number of 500

Figure 9 shows the pressure drop of the fluid in three paths at the Reynolds number of 500. The pressure drop depends on the inlet velocity, friction coefficient, channel length, channel dimensions and the shape of the coolant flow path. The pressure drop becomes greater if the path is twisted under similar conditions. The curved path has more twists compared to

other paths. Therefore, according to Figure 9, the curved path has the most significant pressure drop compared to other paths, followed by the spiral path, which has more curvature than the direct path. At the specified Reynolds number, the pressure drop of the curve path is 260 kPa, which is about 2% and 5% greater than the pressure drop of the spiral (255 kPa) and curved paths (250 kPa), respectively.

5. Conclusion

To enhance the performance of a solar collector, selecting a proper fluid flow path is very important. In this study, three direct, curved and spiral paths are considered for the numerical simulation. It was found that the temperature changes of the coolant passing through the direct microchannel route path at a constant Reynolds number of 500 are greater than temperature variations in the curved and spiral paths. The high temperature of the cell surface because of lower heat exchange between the solar cell and the coolant compared to other paths proves the mentioned issue.

In addition, the highest electrical efficiency, at Re = 500, is related to the curved path, with approximately 12.48%. This amount is 0.5% and 0.8% higher than that of the spiral and direct paths. This stems from the lower surface temperature which results in better cooling potential compared to the other two paths. The more cooling of the solar cell, the higher the electrical efficiency of the solar cell. Moreover, the Nusselt number depends on the convective heat transfer coefficient, which is a function of the temperature difference between the cell surface and the fluid. There is an inverse relationship between the Nusselt number and temperature difference. As long as the temperature difference in the curved path is smaller than that of the other paths, the value of Nusselt number for the fluid in the curved path is 0.14% and 50%more than that of the other paths.

Additionally, the curved path with a pressure drop of 260 kPa has the highest pressure drop in comparison to other paths. This value for the direct and spiral paths is 250 and 255 kPa, respectively. Furthermore, according to the discussed results, it is concluded that if the manufacturers consider electrical efficiency as the most important criterion for the manufacturing of the solar collectors, the curved fluid path is the best choice for them owing to higher electrical efficiency compared to direct and spiral paths .

References

Abdollahzadeh Jamalabadi, M.Y., Safaei, M.R., Alrashed, A.A.A.A., Nguyen, T.K. and Bandarra Filho, E.P. (2017), “Entropy generation in thermal radiative loading of structures with distinct heaters”, Entropy, Vol. 19 No. 10, p. 506.

Agrawal, S. and Tiwari, A. (2011), “Experimental validation of glazed hybrid micro-channel solar cell thermal tile”, Solar Energy, Vol. 85 No. 11, pp. 3046-3056.

Agrawal, S. and Tiwari, G.N. (2015), “Performance analysis in terms of carbon credit earned on annualized uniform cost of glazed hybrid photovoltaic thermal air collector”, Solar Energy, Vol. 115, pp. 329-340.

Babaei, S.M., Razmi, A.R., Soltani, M. and Nathwani, J. (2020), “Quantifying the effect of nanoparticles addition to a hybrid absorption/recompression refrigeration cycle”, Journal of Cleaner Production, Vol. 260, p. 121084.

Bahiraei, M., Mazaheri, N., Aliee, F. and Safaei, M.R. (2019), “Thermo-hydraulic performance of a biological nanofluid containing graphene nanoplatelets within a tube enhanced with rotating twisted tape”, Powder Technology, Vol. 355, pp. 278-288.

Bakhshi, H., Khodabandeh, E., Akbari, O., Toghraie, D., Joshaghani, M. and Rahbari, A. (2019), “Investigation of laminar fluid flow and heat transfer of nanofluid in trapezoidal microchannel with different aspect ratios”, International Journal of Numerical Methods for Heat and Fluid Flow, Vol. 29 No. 5.

Bergman, T.L., Incropera, F.P., DeWitt, D.P. and Lavine, A.S. (2011), Fundamentals of Heat and Mass Transfer, John Wiley and Sons.

Chamkha, A.J., Rashad, A.M., Mansour, M.A., Armaghani, T. and Ghalambaz, M. (2017), “Effects of heat sink and source and entropy generation on MHD mixed convection of a Cu-water nanofluid in a lid-driven square porous enclosure with partial slip”, Physics of Fluids, Vol. 29 No. 5, p. 052001.

Chien, L.-H., Cheng, Y.-T., Lai, Y.-L., Yan, W.-M. and Ghalambaz, M. (2020), “Experimental and numerical study on convective boiling in a staggered array of micro pin-fin microgap”, International Journal of Heat and Mass Transfer, Vol. 149, p. 119203.

Coventry, J.S. (2005), “Performance of a concentrating photovoltaic/thermal solar collector”, Solar Energy, Vol. 78 No. 2, pp. 211-222.

Coventry, J. Franklin, E. and Blakers, A. (2004), “Thermal and electrical performance of a concentrating PV/thermal collector: results from the ANU CHAPS collector”.

Doranehgard, M.H., Samadyar, H., Mesbah, M., Haratipour, P. and Samiezade, S. (2017), “High-purity hydrogen production with in situ CO2 capture based on biomass gasification”, Fuel, Vol. 202, pp. 29-35.

Fudholi, A., Sopian, K., Yazdi, M.H., Ruslan, M.H., Ibrahim, A. and Kazem, H.A. (2014), “Performance analysis of photovoltaic thermal (PVT) water collectors”, Energy Conversion and Management, Vol. 78, pp. 641-651.

Fudholi, A., Sopian, K., Gabbasa, M., Bakhtyar, B., Yahya, M., Ruslan, M.H. and Mat, S. (2015), “Techno-economic of solar drying systems with water based solar collectors in Malaysia: a review”, Renewable and Sustainable Energy Reviews, Vol. 51, pp. 809-820.

Garoosi, F., Safaei, M.R., Dahari, M. and Hooman, K. (2015), “Eulerian–Lagrangian analysis of solid particle distribution in an internally heated and cooled air-filled cavity”, Applied Mathematics and Computation, Vol. 250, pp. 28-46.

Ghalambaz, M., Jamesahar, E., Ismael, M.A. and Chamkha, A.J. (2017), “Fluid-structure interaction study of natural convection heat transfer over a flexible oscillating fin in a square cavity”, International Journal of Thermal Sciences, Vol. 111, pp. 256-273.

Ghale, Z.Y., Haghshenasfard, M. and Esfahany, M.N. (2015), “Investigation of nanofluids heat transfer in a ribbed microchannel heat sink using single-phase and multiphase CFD models”, International Communications in Heat and Mass Transfer, Vol. 68, pp. 122-129.

Hoseinzadeh, S., Ghasemi, M.H. and Heyns, S. (2020), “Application of hybrid systems in solution of low power generation at hot seasons formicro hydro systems”, Renewable Energy, Vol. 160, pp. 323-332.

Hoseinzadeh, S., Ghasemiasl, R., Havaei, D. and Chamkha, A.J. (2018), “Numerical investigation of rectangular thermal energy storage units with multiple phase change materials”, Journal of Molecular Liquids, Vol. 271, pp. 655-660.

Hoseinzadeh, S., Otaghsara, S.M.T., Khatir, M.H.Z. and Heyns, P.S. (2019), “Numerical investigation of thermal pulsating alumina/water nanofluid flow over three different cross-sectional channel”, International Journal of Numerical Methods for Heat and Fluid Flow, Vol. 30 No. 7.

Hosseinzadeh, S., Ostadhossein, R., Mirshahvalad, H.R. and Seraj, J. (2017), “Using simpler algorithm for cavity flow problem”, Mechatronics and Applications: An International Journal (MECHATROJ), Vol. 1.

Jaferian, V., Toghraie, D., Pourfattah, F., Akbari, O.A. and Talebizadehsardari, P. (2019), “Numerical investigation of the effect of water/Al2O3 nanofluid on heat transfer in trapezoidal, sinusoidal and stepped microchannels”, International Journal of Numerical Methods for Heat and Fluid Flow, Vol. 30 No. 5.

Khodabandeh, E., Toghraie, D., Chamkha, A., Mashayekhi, R., Akbari, O. and Rozati, S.A. (2019), “Energy saving with using of elliptic pillows in turbulent flow of two-phase water-silver nanofluid in a spiral heat exchanger”, International Journal of Numerical Methods for Heat and Fluid Flow, Vol. 30 No. 4.

Lee, P.-S. and Garimella, S.V. (2006), “Thermally developing flow and heat transfer in rectangular microchannels of different aspect ratios”, International Journal of Heat and Mass Transfer, Vol. 49 Nos 17/18, pp. 3060-3067.

Li, J., Peterson, G.P. and Cheng, P. (2004), “Three-dimensional analysis of heat transfer in a micro-heat sink with single phase flow”, International Journal of Heat and Mass Transfer, Vol. 47 Nos 19/20, pp. 4215-4231.

Manokar, A.M., Vimala, M., Sathyamurthy, R., Kabeel, A.E., Winston, D.P. and Chamkha, A.J. (2020), “Enhancement of potable water production from an inclined photovoltaic panel absorber solar still by integrating with flat-plate collector”, Environment, Development and Sustainability, Vol. 22 No. 5, pp. 4145-4167.

Meneses-Rodríguez, D., Horley, P.P., Gonz_alez-Hern_andez, J., Vorobiev, Y.V.,. and Gorley, P.N. (2005), “Photovoltaic solar cells performance at elevated temperatures”, Solar Energy, Vol. 78 No. 2, pp. 243-250.

Menni, Y., Azzi, A. and Chamkha, A. (2019), “Modeling and analysis of solar air channels with attachments of different shapes”, International Journal ofNumericalMethods forHeat and Fluid Flow, Vol. 29 No. 5.

Mohammadian, A., Chehrmonavari, H., Kakaee, A. and Paykani, A. (2020), “Effect of injection strategies on a single-fuel RCCI combustion fueled with isobutanol/isobutanol þ DTBP blends”, Fuel, Vol. 278, p. 118219.

Rahbar, N. and Esfahani, J.A. (2013), “Productivity estimation of a single-slope solar still: theoretical and numerical analysis”, Energy, Vol. 49, pp. 289-297.

Rahbar, N., Esfahani, J.A. and Asadi, A. (2016), “An experimental investigation on productivity and performance of a new improved design portable asymmetrical solar still utilizing thermoelectric modules”, Energy Conversion and Management, Vol. 118, pp. 55-62.

Rahbar, N., Esfahani, J.A. and Fotouhi-Bafghi, E. (2015), “Estimation of convective heat transfer coefficient and water-productivity in a tubular solar still – CFD simulation and theoretical analysis”, Solar Energy, Vol. 113, pp. 313-323.

Rahmanian, B., Safaei, M.R., Kazi, S.N., Ahmadi, G., Oztop, H.F. and Vafai, K. (2014), “Investigation of pollutant reduction by simulation of turbulent non-premixed pulverized coal combustion”, Applied Thermal Engineering, Vol. 73 No. 1, pp. 1222-1235.

Razmi, A.R. and Janbaz, M. (2020), “Exergoeconomic assessment with reliability consideration of a green cogeneration system based on compressed air energy storage (CAES)”, Energy Conversion and Management, Vol. 204, p. 112320.

Razmi, A., Soltani, M. and Torabi, M. (2019), “Investigation of an efficient and environmentally-friendly CCHP system based on CAES, ORC and compression-absorption refrigeration cycle: energy and Exergy analysis”, Energy Conversion and Management, Vol. 195, pp. 1199-1211.

Razmi, A., Soltani, M., Kashkooli, F.M. and Garousi Farshi, L. (2018), “Energy and exergy analysis of an environmentally-friendly hybrid absorption/recompression refrigeration system”, Energy Conversion and Management, Vol. 164, pp. 59-69.

Salehi, M., Pourmahmoud, N., Hassanzadeh, A., Hoseinzadeh, S. and Heyns, P.S. (2020), “Computational fluid dynamics analysis of the effect of throat diameter on the fluid flow and performance of ejector”, International Journal of Numerical Methods for Heat and Fluid Flow.

Sarafraz, M., Tlili, I., Abdul Baseer, M. and Safaei, M.R.J.A.S. (2019), “Potential of solar collectors for clean thermal energy production in smart cities using nanofluids: experimental assessment and efficiency improvement”, Applied Sciences, Vol. 9 No. 9, p. 1877.

Shashikumar, N.S., Gireesha, B.J., Mahanthesh, B., Prasannakumara, B.C. and Chamkha, A.J. (2018), “Entropy generation analysis of magneto-nanoliquids embedded with aluminium and titanium alloy nanoparticles in microchannel with partial slips and convective conditions”, International Journal of Numerical Methods for Heat and Fluid Flow, Vol. 29 No. 10.

Sohani, A. and Sayyaadi, H. (2020), “Providing an accurate method for obtaining the efficiency of a photovoltaic solar module”, Renewable Energy, Vol. 156, pp. 395-406.

Sohani, A., Rezapour, S. and Sayyaadi, H. (2020), “Comprehensive performance evaluation and demands’ sensitivity analysis of different optimum sizing strategies for a combined cooling, heating, and power system”, Journal of Cleaner Production, Vol. 279, p. 123225.

Sohani, A., Shahverdian, M.H., Sayyaadi, H. and Garcia, D.A. (2020), “Impact of absolute and relative humidity on the performance of mono and poly crystalline silicon photovoltaics; applying artificial neural network”, Journal of Cleaner Production, Vol. 276, p. 123016.

Teo, H., Lee, P. and Hawlader, MJae. (2012), “An active cooling system for photovoltaic modules”, Applied Energy, Vol. 90 No. 1, pp. 309-315.

Valadez-Villalobos, K., Idígoras, JS., Delgado, L.P., Meneses-Rodríguez, D., Anta, J.A. and Oskam, G. (2019), “Correlation between the effectiveness of the electron-selective contact and photovoltaic performance of Perovskite solar cells”, The Journal of Physical Chemistry Letters, Vol. 10 No. 4, pp. 877-882.

Xu, J., An, B. and Sun, D. (2015), “The phase separation in a rectangular microchannel by micromembrane”, Applied Thermal Engineering, Vol. 88, pp. 172-184.

Xu, J.L., Gan, Y.H., Zhang, D.C. and Li, X.H. (2005), “Microscale heat transfer enhancement using thermal boundary layer redeveloping concept”, International Journal of Heat and Mass Transfer, Vol. 48 No. 9, pp. 1662-1674.

Yan, W.-M., Teng, H.-Y., Li, C.-H. and Ghalambaz, M. (2019), “Electromagnetic field analysis and cooling system design for high power switched reluctance motor”, International Journal of Numerical Methods for Heat and Fluid Flow, Vol. 29 No. 5.

Yarmand, H., Gharehkhani, S., Kazi, S.N., Sadeghinezhad, E. and Safaei, M.R. (2014), “Numerical investigation of heat transfer enhancement in a rectangular heated pipe for turbulent nanofluid”, The Scientific World Journal, Vol. 2014.

Yousef Nezhad, M.E. and Hoseinzadeh, S. (2017), “Mathematical modelling and simulation of a solar water heater for an aviculture unit using MATLAB/SIMULINK”, Journal of Renewable and Sustainable Energy, Vol. 9 No. 6, p. 063702.

Yu, X., Xu, J., Yuan, J. and Zhang, W. (2018), “Microscale phase separation condensers with varied cross sections of each fluid phase: heat transfer enhancement and pressure drop reduction”, International Journal of Heat and Mass Transfer, Vol. 118, pp. 439-454.

Zeynalian, M., Hajialirezaei, A.H., Razmi, A.R. and Torabi, M. (2020), “Carbon dioxide capture from compressed air energy storage system”, Applied Thermal Engineering, Vol. 178, p. 115593.